Anion and Cation Permeability of a Chloride Channel in Rat Hippocampal Neurons

FABIO FRANCIOLINI and WOLFGANG NONNER

From the Department of Physiology and Biophysics, University of Miami, Miami, Florida 33101

ABSTRACT The ionic permeability of a voltage-dependent Cl channel of rat hippocampal neurons was studied with the patch-clamp method. The unitary conductance of this channel was ~30 pS in symmetrical 150 mM NaCl saline. Reversal potentials interpreted in terms of the Goldman-Hodgkin-Katz voltage equation indicate a Cl:Na permeability ratio of ~5:1 for conditions where there is a salt gradient. Many anions are permeant; permeability generally follows a lyotropic sequence. Permeant cations include Li, Na, K, and Cs. The unitary conductance does not saturate for NaCl concentrations up to 1 M. No Na current is observed when the anion Cl is replaced by the impermeant anion SO_4. Unitary conductance depends on the cation species present. The channel is reversibly blocked by extracellular Zn or 9-anthracene carboxylic acid. Physiological concentrations of Ca or Mg do not affect the Na:Cl permeability ratio. The permeability properties of the channel are consistent with a permeation mechanism that involves an activated complex of an anionic site, an extrinsic cation, and an extrinsic anion.

INTRODUCTION

This article examines the ionic selectivity of an anion channel that is consistently found in the somatic membrane of hippocampal neurons from embryonic rats. Characteristic of the channel is a relatively small unitary conductance (~30 pS in symmetrical 150 mM NaCl saline) that is turned on and off by a weakly voltage-dependent, kinetically complex gating process. Activity is strongest at positive voltages, but is maintained to levels as negative as −80 mV. Anion channels with similar overall characteristics have previously been found in the sarcolemma of rat myotubes (Blatz and Magleby, 1985), where they have been suggested to be a molecular basis for the resting Cl conductance of skeletal muscle cells.

When probing the anion/cation selectivity of the channel with a salt gradient, we noticed that several alkali cations, including Na, were significantly permeant. This had been previously noticed for anion channels of large conductance that tend to be closed at potentials distant from zero (Blatz and Magleby, 1983; Gray

Address reprint requests to Dr. W. Nonner, Dept. of Physiology and Biophysics, University of Miami, P.O. Box 016430, Miami, FL 33101. Dr. Franciolini's present address is Istituto Biologia Cellulare, Università di Perugia, 06100 Perugia, Italy.

J. GEN. PHYSIOL. © The Rockefeller University Press · 0022-1295/87/10/0453/26 $2.00

Volume 90 October 1987 453–478

et al., 1984). Blatz and Magleby (1985) found a small-conductance anion channel in myotube that is open at the resting potential; the cation/anion permeability for this channel is ~0.2 when probed with KCl gradients. Thus, a finite cation permeability appears to be a common feature of several anion channels.

Our experiments focused on the mechanism of the dual anion and cation permeability of the neuronal anion channel. The results suggest that the selectivity filter of the channel has the unusual feature that it needs to be complemented by a cation that is adsorbed from the environment. Whereas this cation is essential in mediating anion permeation, it also can become a charge carrier under certain ionic conditions. A preliminary report of some of this work has appeared (Franciolini and Nonner, 1986).

METHODS

The purpose of the experiments was to determine reversal potentials and unitary current-voltage (i-V) relationships for an anion channel in rat hippocampal neurons.

Preparation

The neurons were obtained by dissecting the hippocampal area from rat embryos at day 19 of gestation. The tissue was dissociated mechanically with a plastic pipette, and cells were plated in collagen/polylysine-coated culture dishes containing a basic tissue culture medium (N5) supplemented with a fraction of horse serum (Kaufman and Barrett, 1983). Immunological assays have shown that, in cultures from rat brain stem, these conditions promote survival of neuronal cells (>98%) over that of glial and other cells (Brugge et al., 1985). Measurements were done between days 6 and 21 after plating. The soma of the cells used was phase bright and ~10–20 μm in diameter; the cells fired spontaneous action potentials. All experiments were done at room temperature (~25°C).

Recording Techniques

Unitary currents were measured using the gigaseal patch-clamp technique of Hamill et al. (1981). The pipette was sealed to the somatic part of the neuron, withdrawn from the cell to excise a membrane patch in the inside-out configuration, and transferred while immersed in saline into a microchamber. Fig. 1 shows the essential part of this chamber. A perfusion canal was formed between a coverslip bottom and a Perspex top, joined by a layer of silicon resin. A 300-μm hole, drilled through the Perspex ceiling of the canal, was covered by a 5-μm-thick polyester filter membrane (Nucleopore Corp., Pleasanton, CA), which was sealed to the Perspex by Vaseline. The tip of the patch pipette was inserted ~10 μm deep into one of the 10-μm holes of the filter membrane, and the saline above the level of the membrane was removed by suction. The canal was continuously perfused with saline and drained by gravity flow so that a negative pressure was maintained near the pipette tip. With the pipette resting on the edge of the small hole, the arrangement provided mechanical stability and efficient perfusion. It also minimized the electric capacity between the pipette and bath solutions by removing the saline surrounding the shaft of the glass pipette. We found this technique for reducing capacity superior to the usual resin-coating of pipettes.

The electrodes in contact with the pipette and bath solutions were protected against effects of Cl substitution. Both electrodes were made of Ag/AgCl pellets. The bath electrode was mounted in an inner chamber that was perfused with a Cl saline under positive pressure; its outer chamber, represented by the outflow canal of the perfusion chamber, was separated from the inner chamber by a filter membrane of 0.1 μm pore

size. The pipette electrode was attached with epoxy glue to one end of a 3-cm-long glass capillary that was filled with a Cl saline and inserted into the patch pipette. The offset voltage between the electrodes was measured before and after each experiment; it typically drifted by <1 mV. Junction potentials were measured for each solution (with respect to a sleeve-type calomel reference electrode; 476012, Corning Medical, Medfield, MA) and used to correct the readings of membrane potential.

The current-to-voltage converter for measuring pipette current used a feedback resistor of 5 GΩ; its frequency response was boosted to a bandwidth of >10 kHz. The current signal was usually filtered through two four-pole Bessel-like low-pass filters (overall 3 dB attenuation at 446 Hz) and digitized at intervals of 500 μs. Command voltages were generated through a homemade digital stimulator that was controlled through a minicomputer (Nova 4 [Data General, Westboro, MA] or an LM2 lab computer provided to us by Dr. Kehl's group at the University of Washington, Seattle, WA). The computer received and stored the samples of patch current on digital magnetic tape.

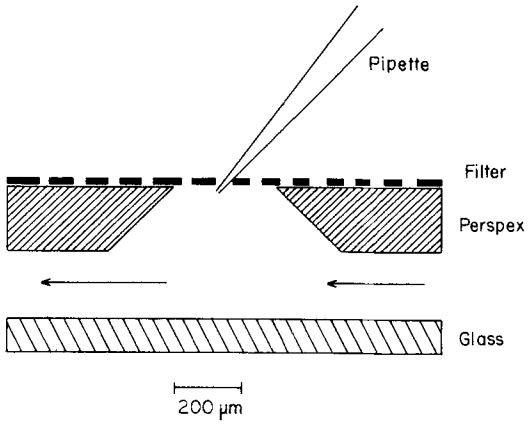

FIGURE 1. Schematic diagram of the perfusion microchamber. The filter membrane and pipette are not drawn to scale; the holes in the filter were ~10 μm in diameter; the membrane was 5 μm thick. This cross section shows only a small part of the arrangement, which was built on a 24- × 50-mm coverslip. The excised patches were transferred from a bath in a different section of the coverslip, where segments of culture dishes containing the neurons were kept.

Stimulation Protocol

The anion channel, as will be described later, is preferentially active during depolarization. In order to record an adequate number of unitary events at all voltages of interest, we stimulated the membrane with a staircase pattern of voltage steps (Fig. 2*A*) that started with positive-going steps to activate channels, followed by negative-going steps applied over a period during which sufficient activity was sustained. The pattern was designed such that each voltage level to be scanned was visited twice, once by an upward step and once by a downward step of equal amplitude. The membrane current was sampled from 50 ms after the onset to the end of each step. Transients of background current that had not settled after the 50-ms blanking periods were eliminated during the later analysis by algebraically adding the corresponding samples of the first and second scanning of each

voltage level. A run for measuring the *i-V* relationship in a given test saline included 10–20 sweeps through the staircase pattern, spaced at 3–5-s intervals. The first sweep was taken at a low gain to determine the size of the currents; the computer then determined the adequate amplification and set a variable-gain amplifier for recording the sweeps to be saved. During the pauses between sweeps, the membrane voltage was maintained at zero.

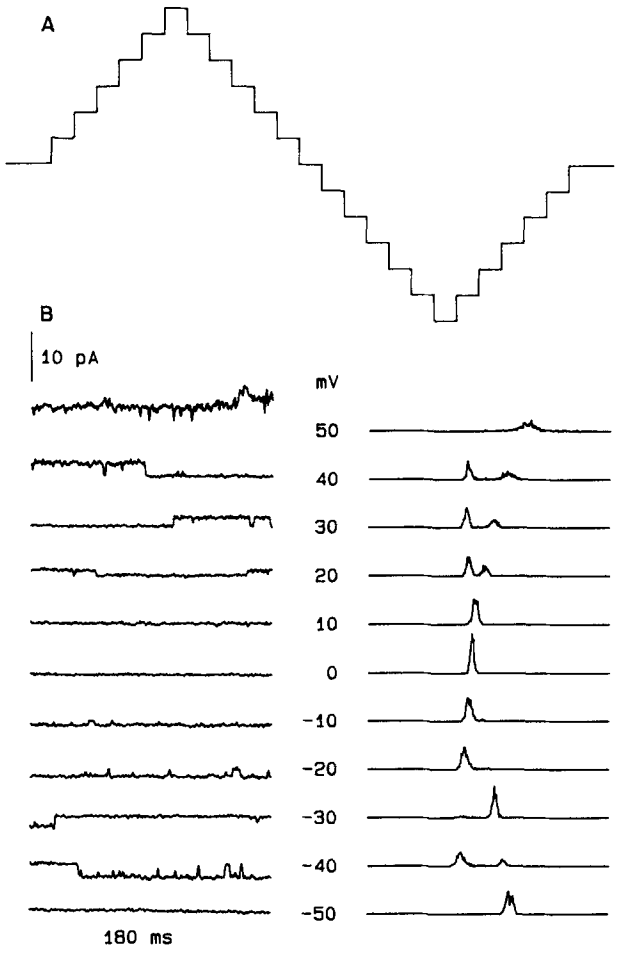

FIGURE 2. Measurement of unitary *i-V* relationship. (*A*) Staircase voltage pattern applied to the patch membrane. Each step lasts 230 ms, and steps are spaced at 10-mV increments. (*B*) On the left are current traces obtained at the different voltage levels of the staircase. Corresponding samples from the first and second visit to each voltage level were algebraically added; the sum is shown. On the right are amplitude histograms from the traces on the left. The abscissa spans 10 pA and is roughly centered to contain the current range of interest (the seal current peaks have not been lined up). The ordinate plots the square root of the number of samples in each bin. This experiment was done with symmetrical 300 mM NaCl saline.

Analysis

The minicomputer was used to analyze the current samples. In an initial, automatic procedure, it sorted, calibrated, and algebraically added the samples from up and down steps to each voltage. The extrema of the currents were determined and used to compute an approximate leak conductance. Currents were corrected for this leak and amplitude

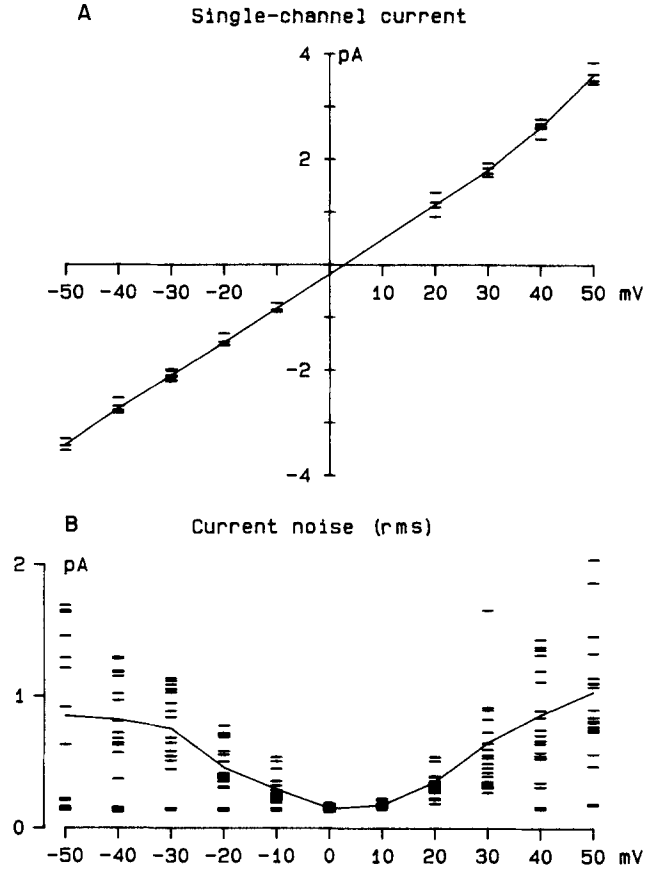

FIGURE 3. Unitary current (*A*) and rms of patch current (*B*) vs. voltage. Estimates from individual staircase sweeps are marked as horizontal bars. The line plots the average. The rms plot was used as a control for reversal potential estimates in experiments that gave small unitary currents. Same experiment as in Fig. 2.

histograms were computed over the range spanned by the unitary events, as illustrated in Fig. 2*B*. In addition, the computer calculated the rms values of the current samples at each voltage and their averages (Fig. 3*B*).

The second part of the analysis was done in an interactive way. For a quick determination of reversal potentials, the minimum of the rms vs. voltage curve (Fig. 3*B*) was determined by a least-squares interpolation (using the square root of a parabola, fitted to the five or six points enclosing the minimum of the rms curve).

For a more thorough analysis in terms of the unitary *i-V* curve, the following procedure was employed. The net current traces from the different voltages of a sweep were displayed together with their corresponding amplitude histograms. For each voltage at which channel openings or closures occurred, the histogram peaks to be analyzed were designated by moving a crosshair cursor and specifying the order of the current level. The computer then calculated the average current corresponding to the peak (using all samples falling into the window defined by the intersections of the horizontal bar of the cursor and the histogram peak). The current level thus determined was indicated in the histogram as well as in the display of sampled current as a control. The computer determined the unitary current from the differences of the identified current levels. This current was inserted into an accumulated scattergram of the single-channel *i-V* curve (Fig. 3*A*), which was also displayed during the analysis. Finally, an average *i-V* curve was calculated from the results of all recorded sweeps.

Solutions

Intracellular and extracellular salines usually contained the specified concentration of bulk salt, 2 mM morpholinopropanesulfonic acid (MOPS), and 1 mM EGTA, adjusted to pH 7.2 by addition of the hydroxide of the bulk cation. These standard solutions will be referred to as, e.g., 300 mM CsCl saline. Note that the standard solutions did not include an addition of divalent cations. We chose this approach to avoid reactions between divalent cations and some anions to be tested. The effects of divalent cations were examined in separate experiments, as described in the Results. Wherever the solutions used did not have the standard composition, it will be explicitly mentioned in the text. The following reagents were used in preparing solutions containing organic bulk anions: L-glutamic acid (99%), acetic acid (99%+), and benzoic acid (99%+) from Aldrich Chemical Co., Milwaukee, WI; L-aspartic acid from Sigma Chemical Co., St. Louis, MO; and propionic acid (99.6%) from Baker Chemical Co., Phillipsburg, NJ. The blocking agent 9-anthracenecarboxylic acid (9-ACA, 98%) was purchased from Aldrich Chemical Co.

General Properties of the Anion Channel and Other Channels

Anion channels of the kind described here were found in the majority of membrane patches excised from hippocampal neurons of various shapes (granular, bipolar, and pyramidal), but also in cultured neurons from other areas (basal ganglia, cortex, spinal cord). We studied the permeability of the channel in hippocampal neurons of unselected morphology. With pipettes of 4–10 MΩ resistance in 150 mM NaCl saline, the patches frequently contained two or more channels. The number of active units tended to increase while measurements were performed on the excised membrane patch. This was fostered by several kinds of manipulation that were necessary during our experiments: application of positive (>30 mV) voltages over several seconds, exposure to hypertonic solutions (by addition of salt or nonelectrolyte), and exposure to some highly permeant anions (such as iodide). On the other hand, the channel activity was not significantly modulated by internal Ca or Mg (up to 2 mM) or by external application (to outside-out patches) of the transmitters γ-aminobutyrate (10 μM) or glycine (10 μM).

Under the experimental conditions used in most of the experiments (zero holding potential, Ca- and K-free salines), the excised membranes revealed little activity from channels other than the 30-pS anion channel. We occasionally observed a large-conductance anion channel, or an ~30-pS cation channel whose gating was characterized by a rapid flicker. These channels were clearly distinguishable from the 30-pS anion channel. Membrane patches containing such channels were rejected.

RESULTS

Characteristics of the Anion Channel

Fig. 4 shows records from an excised inside-out patch that contained a single unit of the anion channel studied in this article. The traces in *A* were measured while both sides of the membrane were exposed to 150 mM NaCl saline; the traces in *B* were measured after switching to an internal solution of 100 mM Na_2SO_4. The membrane voltage was changed by manually switching the holding potential between +40, 0, and −40 mV at tens of seconds before the currents were sampled. With Cl ions present on both sides, unitary events were observed at either polarity of the voltage. After SO_4 was substituted for internal Cl, the

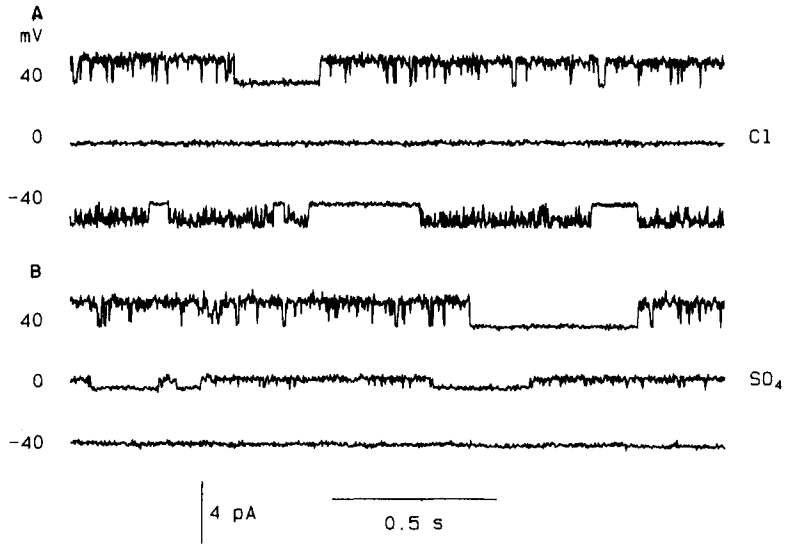

FIGURE 4. Unitary currents from an anion channel at three maintained voltages. An excised inside-out patch was used; the pipette contained 150 mM NaCl saline; the bath solution was 150 mM NaCl (*A*) or 100 mM Na_2SO_4 saline (*B*). This and all other recordings in this article were low-pass-filtered at 446 Hz; the temperature was ~25°C.

inward-going events were abolished as expected if Cl, but not SO_4 or Na, supports current in these channels. In other experiments described below, substitution of Na ions by other alkali cations (e.g., Cs; Fig. 5) had no obvious effect on the unitary current in these channels. These preliminary experiments suggest that Cl is the major charge carrier. The top trace of Fig. 4 indicates a unitary chord conductance of 35 pS for a symmetrical 150 mM NaCl bathing solution.

Fig. 5 shows that two agents that have been found to block Cl currents in other preparations, external Zn and 9-ACA (Stanfield, 1970; Bryant and Morales-Aguilera, 1971; Woodbury and Miles, 1973; Palade and Barchi, 1977), also act on the anion-selective channels studied here. These experiments were done on outside-out patches. Adding 1 mM $ZnCl_2$ to an external CsCl saline abolished

the current (Fig. 5*A*); the effect was completely reversible (not shown). A 1-mM dose of 9-ACA introduced flickering and also reduced the overall current. The strength of the effect depended on transmembrane voltage: the block was more pronounced at +20 than at −20 mV. The block by 9-ACA was reversible, as well (not shown).

As can be seen from the recordings presented so far, current through the anion channels is modulated by a gating process with complex kinetics. Openings typically occur in bursts that last for a fraction of a second and contain many short closures. Opening activity is enhanced as the membrane voltage is shifted in the positive direction. In the records of Fig. 4*A*, the fraction of time attributable to the bursts of openings increased from 0.62 to 0.89 upon changing the voltage from −40 to +40 mV; the average burst and interburst intervals were 0.11 and 0.17 s for −40 mV, and 0.63 and 0.26 s for 40 mV. We note that sustained single-unit openings were observed under conditions where the open probability was high; hence, this kind of anion channel does not appear to occur in multiples of two units (Miller and White, 1984).

We have done control experiments to examine whether the short closures during bursts of openings are related to the presence of EGTA and MOPS buffers in the test salines. Reducing the concentration of either buffer 10-fold with respect to its usual level (1 mM EGTA, 2 mM MOPS; see Methods) did not significantly alter the frequency of short closures or enhance the apparent unitary conductance. However, an additional degree of flicker and a depression of the conductance were observed with 10 mM EGTA or 20 mM MOPS. The concentrations of EGTA and MOPS used during most of this work thus do not seem to interfere with the measurements of bulk ion permeability. On the other hand, the presence of brief closures (and other fast events that give rise to the noise seen during the open periods) complicates measurements of unitary current in this channel. The estimates of unit conductance reported here refer to openings that were sufficiently long to be resolved at a bandwidth of ~450 Hz (see Methods).

Anion vs. Cation Selectivity

The reversal potential measurements presented in this section show that although the channel is preferentially selective for Cl, it also has a permeability to alkali cations. The unitary *i-V* curves presented in Fig. 6 were obtained from an inside-out patch that was sequentially perfused with 300, 75, 300, 150, 300, and 1,000 mM NaCl salines; the pipette contained 1,000 mM NaCl solution. The membrane patch was stimulated by a staircase pattern of voltages, and unitary currents were determined as described in the Methods. With any of the 75, 150, or 300 mM salines on the inside, the net current at zero voltage was outward; hence, Cl was the main carrier of charge. The reversal potentials, however, shifted to a lesser extent than expected for an ideal Cl electrode. For instance, in the case of the 150 mM internal saline, one would expect the Nernst potential to be −44 mV (using activity coefficients of 0.756 and 0.657 for the 150 and 1,000 mM salines), whereas the actual reversal potential was near −36 mV. The difference is not

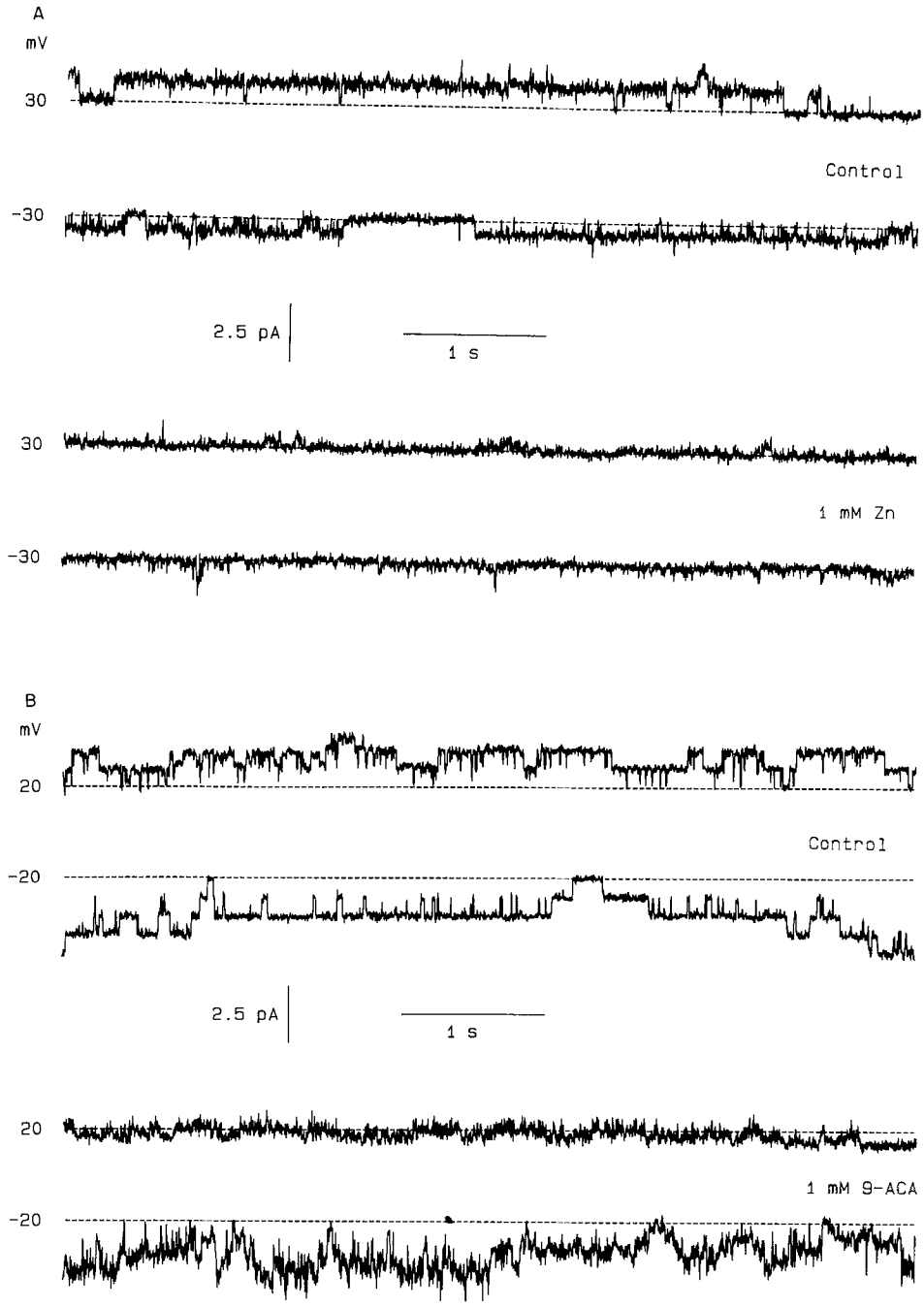

FIGURE 5. Block of anion channels by 1 mM external Zn (*A*) or 1 mM external 9-ACA (*B*). Two different outside-out patches were used. The bath solution was symmetrical 150 mM CsCl salines at pH 7.0 (*A*) or 7.2 (*B*).

attributable to junction potentials, which were measured and corrected for as outlined in the Methods; it is several times larger than the scatter among reversal potentials obtained from the repeated runs in the 300 mM saline (see Fig. 6). Indeed, deviations from the Nernst slope were found consistently in experiments of this kind. An overview of these results is shown in Fig. 7. The open symbols plot measured reversal potentials from individual runs against the activity ratio of the internal and external salines. The closed symbols represent the averages of many determinations as detailed in the legend. The longer dashed straight line is calculated from the Nernst equation. The shorter dashed curve plots the prediction of the Goldman-Hodgkin-Katz (GHK) voltage equation for the case of $P_{Na}/P_{Cl} = 0.2$. The fit with this curve is reasonable over two decades of activity

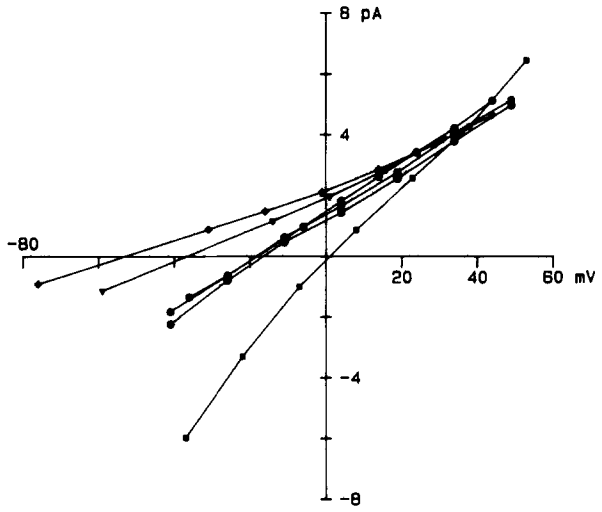

FIGURE 6. Test for anion/cation selectivity. Unitary *i-V* curves from a single inside-out patch obtained through the staircase method illustrated in Figs. 2 and 3. The pipette contained 1 M NaCl saline; the bath salines contained NaCl at 75 mM (◆), 150 mM (▼), 300 mM (●, three curves), or 1 M (■). The sequence of bath solutions was 300, 75, 300, 150, 300, and 1,000 mM.

ratios, so the results of these reversal potential measurements are roughly consistent with an anion/cation selectivity ratio of 5:1. The deviations from the Nernst potential do not vary in size upon reversing the salt gradient; apparently the channel has no significant asymmetry with regard to the anion/cation discrimination.

Since the protocol of these experiments implied osmotic gradients across the membrane, we have to consider two other possible interpretations of the results, which do not require that Na ions be permeant in the anion channel. (*a*) The deviations from the Nernst potential for anions reflect a streaming potential caused by mutually interdependent fluxes of anion and water in a narrow pore. (*b*) The actual anion gradient between the unstirred layers near the membrane is smaller than the bulk gradient because water is moving through the lipid phase

(thus producing a "dilution potential"). Both effects would act to reduce reversal potential shifts produced by salt gradients across an anion-selective channel.

In order to detect such osmotic effects, we examined whether the reversal potential was shifted when an osmotic gradient was created by unilateral addition of nonelectrolyte. Addition to the internal saline of 1 M sucrose, glucose, glycerol, or urea was accompanied by small (−0.5 to +1.5 mV) variations from the reversal potential measured with the symmetrical 300 mM NaCl salines. This puts an upper limit on the combined effects of streaming potential and water flux. For comparison, increasing the internal NaCl concentration from 300 mM to 1 M

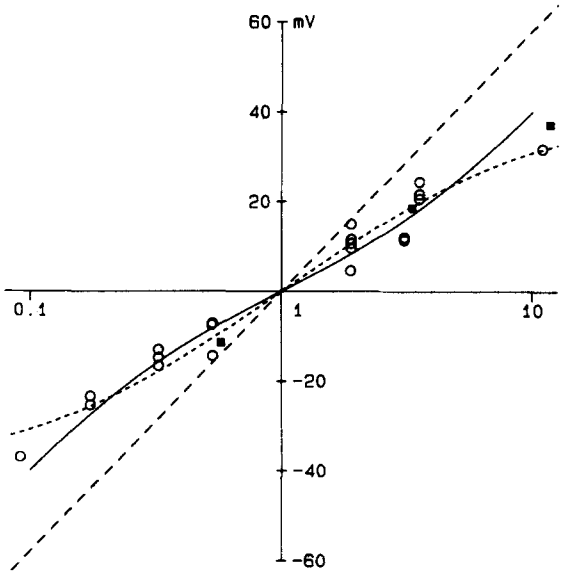

FIGURE 7. Reversal potential vs. NaCl activity ratio. The open circles refer to results from individual patches including the one in Fig. 6. The filled squares mark averages obtained for frequently used activity ratios from a different group of patches (N = 8, 21, and 4 for activity ratios 0.576, 3.33, and 11.77, respectively). The longer dashed line indicates the Nernst potentials for Cl ions. The shorter dashed curve is drawn from the GHK voltage equation assuming a cation/anion permeability ratio of 0.2. The solid curve plots reversal potentials computed for Eq. 1 of the Appendix, with $k_{31}/k_{32} = 1$ (see Discussion).

shifted the reversal potential by 18.5 mV, which is 12.4 mV less than the Nernst potential change for Cl (this is the condition for which the largest number of measurements were done; see the legend to Fig. 7). We conclude that the observed difference cannot be attributed to the presence of an osmotic gradient during our experiments.

This view is further supported by relevant experiments reported in the literature, which bear on the size of dilution potentials. Blatz and Magleby (1984, 1985) found that currents through Ca-activated K channels in excised membrane patches of myotube reverse near the Nernst potential for K in the presence of

osmotically uncompensated salt gradients (up to 1 M vs. 100 mM KCl). They report that in patches where both K and Cl channels were present, the reversal potentials of the Cl channel significantly deviated from the Nernst potential, whereas those for the K channel did not. In experiments with artificial lipid bilayers, Rosenberg and Finkelstein (1978) found that with, e.g., 100 mM KCl in one bath and 100 mM KCl plus 2 M urea in the other, valinomycin-induced currents reversed at 0.6 mV (unstirred baths) to −1.2 mV (stirred baths); in a control experiment, a K-selective electrode measured a difference of −2 mV when moved from 100 mM KCl to 100 mM KCl plus 2 M urea.

Together, these experiments and our own controls indicate that streaming potentials or dilution by water flux cannot account for the observed differences

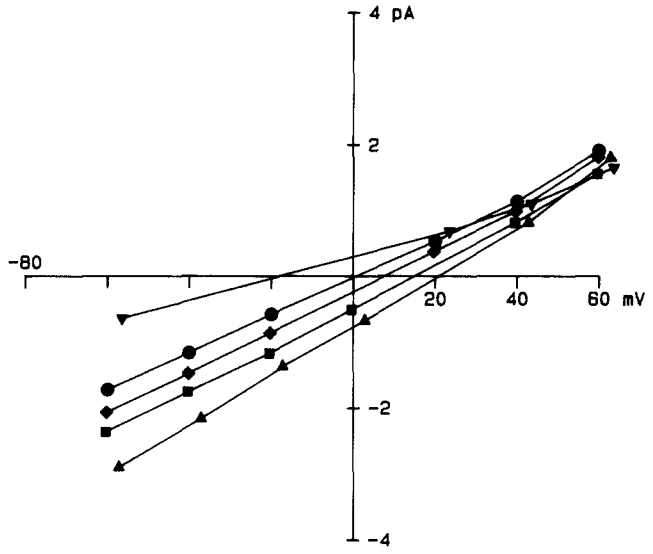

FIGURE 8. Test of halide and NO_3 anion permeability. A single inside-out patch was internally bathed in a sequence of 150 mM salines containing the Na salts of F (▼), Cl (●), Br (◆), I (■), or nitrate (▲); the pipette contained a 150 mM NaCl saline.

between reversal potentials and the Cl Nernst potential. By exclusion, we suggest that the Cl channel has a significant permeability to Na cations.

The following sections report experiments to further characterize the channel's ability to conduct both anions and cations. We first survey ionic selectivities among different species of anion and cation, using reversal potential measurements as the indicator of permeability.

Selectivity among Anions

All of the halide anions are permeant in the anion channel. This is demonstrated by the family of *i-V* curves in Fig. 8. The pipette solution for this patch was the 150 mM NaCl saline; five internal anions were tested under biionic conditions: F, Cl, Br, I, and NO_3. The reversal potential for F is negative, which indicates

that F is less permeant than Cl. The reversal potentials for Br, I, and NO_3 are positive and increase in this order. These ions are preferred over Cl to an increasing extent.

Table I summarizes this and other biionic substitution experiments with halides and other anions in terms of permeability ratios. These ratios were derived through an appropriate version of the GHK voltage equation, which considers the contributions from Na, Cl, and the test ion. The ratio P_{Na}/P_{Cl} was assumed to be 0.2, as suggested by the experiments in the preceding section, and was taken to be independent of the test ion species. The experiments with organic

TABLE I

Reversal Potential Shifts and Permeability Ratios

Test ion	ΔE_{rev}	N	P_{test}/P_{Cl}
	mV		
Glutamate	−32.5	3	0.13
Aspartate	−29.6	3	0.17
F	−15.7	2	0.44
Propionate	−13.4	2	0.5
Acetate	−8.5	5	0.66
Cl	0	—	1
SCN	7.9	1	1.44
Br	8.2	2	1.46
Benzoate	13.6	2	1.86
I	15.0	2	1.98
Nitrate	19.0	2	2.35
Li	−3.7	7	0.38
Na	0	7	0.25
K	−1.1	3	0.25
Cs	−6.2	2	0.35

Reversal potential shifts are with respect to the control NaCl saline. In the anion experiments, the pipette contained 150 or 300 mM NaCl; the bath solution contained the Na salt of the test anion at the same concentration. During cation experiments, the pipette saline was 300 mM NaCl, whereas the bath contained a 1 M solution of the Cl salt of the test cation. Permeability ratios are calculated from: $E_{rev} = RT/F \ln[(P_{Na}\, a_{Na,o} + P_A\, a_{Ai})/(P_C\, a_{Ci} + P_{Cl}\, a_{Cl,o})]$, where P_{Na}/P_{Cl} is taken to be 0.2 for the anion substitution experiments, or is computed from the controls with Na saline in the cation substitution experiments. "A" and "C" denote the anion and cation in the (cytoplasmic) test saline. Activities were taken from the tables of Robinson and Stokes (1959).

ions were done with 300 mM solutions since they produced relatively small unitary currents; inorganic ions were tested with 150 mM solutions.

Overall, the monovalent anion permeabilities follow the lyotropic sequence. We also tested one divalent anion, SO_4; it shifted the reversal potential by at least 50 mV in the negative direction (a reversal of unitary current could not be detected as there was no identifiable activity in the inward direction; see Fig. 4*B*). This places SO_4 at the low-permeability end of Table I, as is appropriate for a lyotropic sequence. Among the organic anions tested, the ion with the

largest hydrophobic group (benzoate) is preferred over species that have fewer hydrocarbons (e.g., propionate) or possess hydrophilic groups in addition to the carboxylic group (e.g., glutamate).

Selectivity among Cations

We tested four alkali cations, Li, Na, K, and Cs, and found all of them to be permeant. With 300 mM NaCl saline in the pipette and 300 mM LiCl, NaCl, KCl, or CsCl in the bath solutions, the reversal potentials were indistinguishable. However, significant differences were seen when 1 M test salines were used in

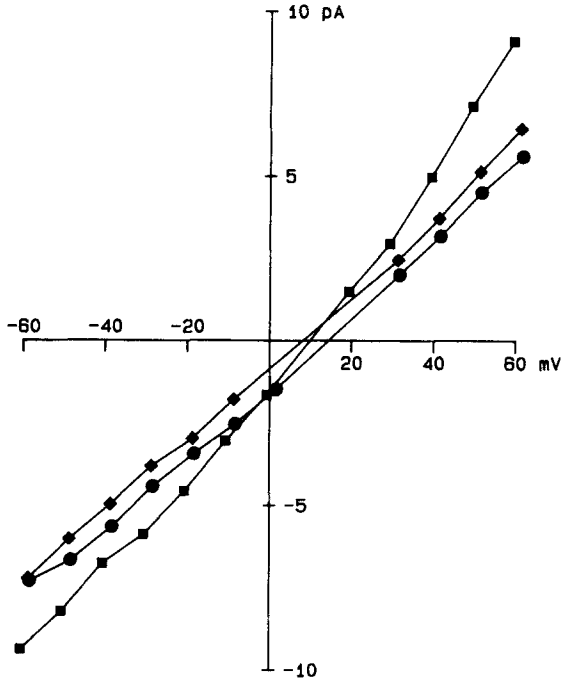

FIGURE 9. Effects of varying the internal cation. *i-V* relationships were obtained from a single patch with 1 M LiCl (◆), NaCl (●), and CsCl (■) in the intracellular bath; the pipette solution was 300 mM NaCl saline.

the bath, and 300 mM NaCl was in the pipette. Fig. 9 shows *i-V* curves from one of these experiments; Table I summarizes the reversal potential shifts and permeability ratios computed using the GHK voltage equation. The permeabilities to Na and K are similar, whereas the permeabilities to Li and Cs are higher than those for Na or K.

Unitary Conductance

In surveying the conductance properties of the channel, we addressed three questions: (*a*) Does the unitary conductance saturate with increasing salt concentration? (*b*) Do cations carry current to the extent suggested by their effects on

the reversal potential? (*c*) Does the channel transport cations and anions independently of each other?

The unitary conductance measured with symmetrical salines increased in approximate proportion to activity if the NaCl concentration was raised from 150 to 300 mM. The average conductances were 30.8 pS at 150 mM ($N = 8$, SEM = 0.7) and 64 pS at 300 mM ($N = 35$, SEM = 0.9). Hence, the conductance ratio was 2.08. The ratio of salt activities was ~1.88 for this case (Robinson and Stokes, 1959). Increasing the NaCl concentration to 1 M further increased the conductance to 130 pS ($N = 2$). This increase is less than proportional (the activity was raised approximately threefold, whereas the conductance increased only twofold with respect to 300 mM) and may indicate that the channel conductance begins to saturate at salt concentrations well above the physiological range.

We attempted to detect current attributable to Na cations after substituting an impermeant anion for Cl. With Na_2SO_4 in the bath facing the cytoplasmic surface and NaCl in the pipette (see Fig. 4), resolvable unitary currents were always outward (Fig. 10*A*, squares). Conversely, no outward current was observed at positive potentials when Na_2SO_4 bathed the extracellular surface and NaCl bathed the cytoplasmic surface (Fig. 10*A*, diamonds). Substituting SO_4 for Cl on both sides eliminated any resolvable unitary events; the rms of the patch current noise in this kind of experiment is plotted vs. voltage in Fig. 10*B*. The circles refer to the control (with internal Cl); the squares refer to the noise after internal Cl was substituted by SO_4. The rms current with the symmetrical SO_4 saline is close to the background noise seen in patches that did not contain channels.

One explanation for this failure to detect cation current may be that SO_4 acts as a potent blocker of the anion channel. This possibility is not supported by the currents in Figs. 4 and 10*A*: the outward current after substituting SO_4 for internal Cl is at all voltages equal to or larger than it was in the control with internal saline. If SO_4 were a blocker, one would have expected some degree of block from the high concentration of internal SO_4 even at voltages unfavorable to the entry of SO_4 anion. Signs of block were absent also in other experiments in which 25 or 50% of the internal Cl was replaced by SO_4. Adding 100 mM Na_2SO_4 to the normal 150 mM NaCl saline in the internal bathing solution (Fig. 10*C*) did not affect the unitary currents: the *i-V* curves before and after SO_4 addition were nearly superimposable. Furthermore, if SO_4 were a blocker and were excluded from its site of action by Cl, the site would have to be occupied for most of the time by a Cl ion; at least for a simple channel with a single anion-binding site, this is inconsistent with the lack of saturation found in measurements already described. Altogether, our attempts to detect a blocking effect of SO_4 were unsuccessful. We are left with the conclusion that the channel conducts cations only when permeant anions are present and are likely to access the channel.

The idea that anions and cations interact while they pass through the channel was supported by an additional observation. When we substituted other alkali ions for internal Na ions (Fig. 9), the size of the unitary currents depended on the cation species. In particular, the internal presence of Cs ions increased the

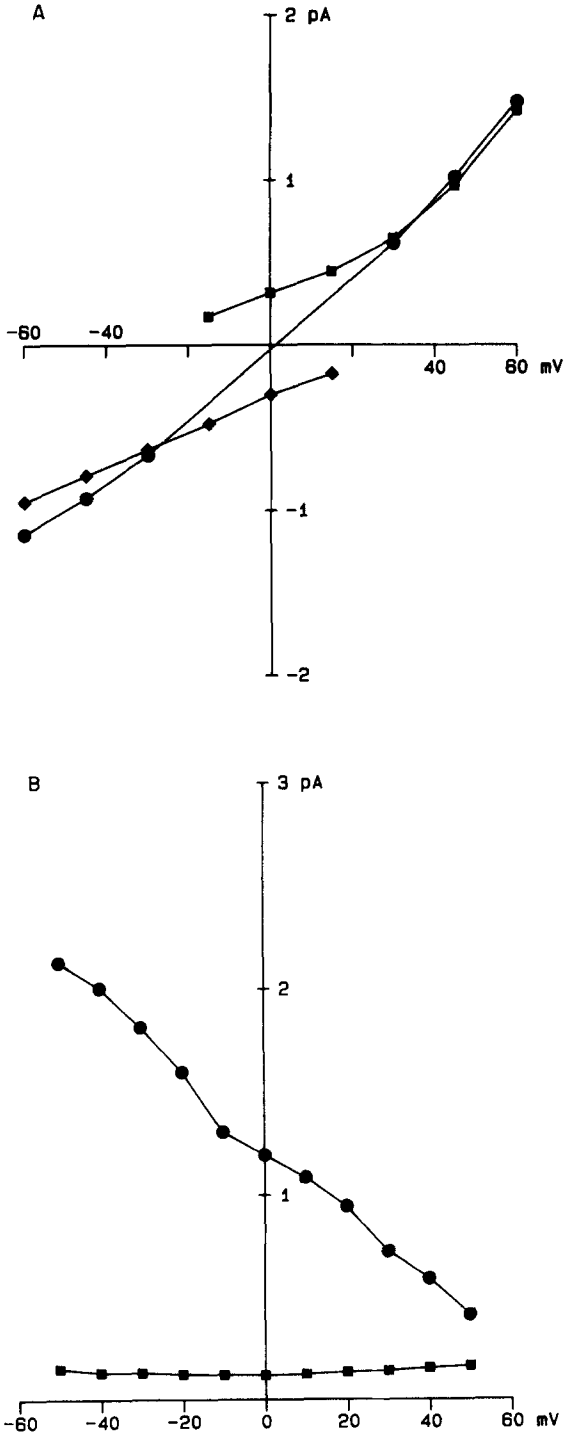

FIGURE 10.

unitary conductance ~1.4-fold relative to the control with Na. The conductance-enhancing effect is different from the effect expected if Cs simply contributes more current than does Na (as may be supposed from the higher permeability of Cs; see Table I). Addition of an outward Cs current would have increased outward current but decreased inward current, which was not observed. The observed increase in unitary conductance is instead consistent with the hypothesis that the cation bound to the channel affects the passage of anions. A mechanistic model of this kind is developed in the Discussion.

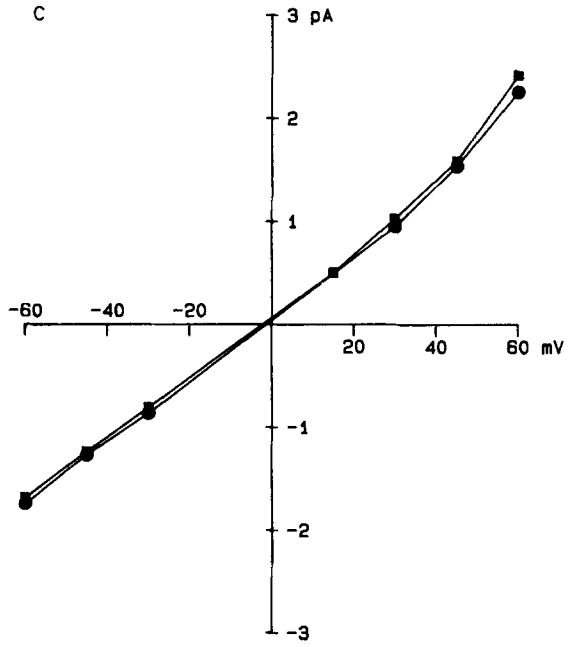

FIGURE 10. (*A and B opposite*) Tests for SO_4 ion permeation or block. (*A*) Unitary currents from two different patches vs. voltage. Symbols: before (●) and after (■) substituting 100 mM Na_2SO_4 for 150 mM NaCl internal saline; external saline was 150 mM NaCl; (◆) from a different patch bathed in 150 mM internal NaCl and 100 mM external Na_2SO_4 saline. (*B*) rms of patch current vs. voltage. From an inside-out patch, with 100 mM Na_2SO_4 in the pipette. Internal salines were 150 mM NaCl (●) or 100 mM Na_2SO_4 (■). (*C*) Unitary current vs. voltage. Symbols: symmetrical 150 mM NaCl salines (●); after changing internal saline to 150 mM NaCl plus 100 mM Na_2SO_4 (■).

Divalent Cations Do Not Affect Permeability

Since all of the experiments described so far were done with salines that were free of added divalent cations and contained EGTA, we had to test for possible effects of divalent cations in separate experiments. We chose to do this control in the presence of a large NaCl gradient, because adsorption of divalent cations to the channel is likely to affect the cation/anion permeability ratio and hence to produce observable shifts of reversal potential under these conditions. The

results, summarized in Table II, show that 1 mM Ca and/or 1 mM Mg, added on either side or both, did not significantly shift the reversal potential. Furthermore, the size of the unitary currents was not measurably altered. We conclude that the absence of physiological concentrations of divalent ions did not bias our results on channel permeability. If the channel binds cations, it prefers monovalent bulk cations over divalent cations at a concentration of 1 mM. This lack of effect of Ca and Mg is in contrast to the blocking effect seen at a low concentration of Zn (Fig. 5*A*). It appears that the channel's preference for Zn does not imply a preference for a twofold positive charge.

TABLE II

Experiments with Divalent Cations

NaCl	Divalent cation	E_{rev}	SE	E_{Cl}
		mV		*mV*
150//2,000	—	38.0	0.4	63.2
	Ca//—	36.4	0.3	—
300//1,000	—	18.7	1.2	30.9
	—//Mg	20.0	1.1	—
	Ca//—	17.5	1.8	—
300//150	—	−11.1	0.9	−14.1
	—//Mg	−11.0	1.8	—
	Ca//—	−12.8	—	—
	Ca//Mg	−11.9	—	—

Divalent cations were added at a concentration of 1 mM. The monovalent ion concentrations are in millimolar (external//internal).

DISCUSSION

We have studied the permeability properties of a Cl channel present in the somatic membrane of hippocampal neurons cultured from rat embryo (day 19). The channel lacks sensitivity to transmitters known to activate other Cl channels and is active over a wide range of membrane potentials, which may suggest that it plays a part in the background conductance of the hippocampal neurons. Indeed, blockers of resting Cl channels in skeletal muscle, Zn and 9-ACA, are also blockers of this neuronal anion channel.

Ionic Selectivity

Reversal potentials indicate that the channel selects among halide ions in the sequence I > Br > Cl > F (Fig. 7) in the ratio 1.98:1.46:1:0.44 (Table I). This is the first of Eisenman's (1965) anion selectivity sequences, which is predicted if the anion interacts with a cationic site of low electric field strength (effective radius >1.8 Å). When the other anions tested are included, the selectivity sequence becomes: NO_3 > I > benzoate > Br > SCN > Cl > acetate > propionate > F > aspartate > glutamate > SO_4. This sequence is within the range of sequences referred to as lyotropic or chaotropic (Hofmeister, 1890), which rules the efficacy of anions in a large variety of physicochemical phenomena. Examples concerning anion-protein, anion-phospholipid, and anion-air/water interface in-

teractions have been recently reviewed in Dani et al. (1983). Lyotropic adsorption in model systems appears to be fostered by the simultaneous interaction of the anion with an electric charge or dipole and neighboring hydrophobic groups (cf. Dani et al., 1983). The observed high permeability to benzoate and the potent blocking effect of 1 mM 9-ACA are consistent with a hydrophobic moiety in the anion channel. Carboxylic acids with less hydrophobic residues, such as acetate, aspartate, and glutamate, accordingly have smaller permeabilities than benzoate. Whereas some of the large lyotropic anions are known to cross lipid membranes per se, the fairly large permeability to a small anion like F suggests that favorable electrostatic interactions are also involved. We thus find support for both kinds of groups typically present in a lyotropic site.

If the ionic pathway has this kind of structure, it would be expected to impede the passage of alkali cations. By contrast, we find that Cs, K, Na, and even Li ions are permeant (Table I). Their permeabilities (Li ~ Cs > K ~ Na) reveal an unusual sequence. The channel rejects the major physiological alkali cations, Na and K, more strongly than the smaller Li or the larger Cs. This is not an Eisenman sequence, but it could in principle be produced by a series of Eisenman "filters" (Eisenman and Horn, 1983), i.e., by successive electrostatic interactions with several groups that individually would give rise to mutually opposite Eisenman sequences. In any case, it appears highly unlikely that these alkali cations could be accommodated by a channel that lacks an anionic site. Such a site, however, would be expected to reject anions from the channel, which is not observed. This difficulty in interpreting our results has led us to consider the possibility that one of the charged species, anion or cation, can enter the channel only when a permeant ion of opposite charge is already in the channel and helps attract the other ion as a counterion. A simple hypothesis of this kind is worked out below and is shown to be generally consistent with our observations.

Comparison with Previous Work on Anion Selectivity

Table III compares anion selectivity ratios from two other studies with this work. The first study (Woodbury and Miles, 1973), on frog skeletal sarcolemma, is based on measurements of resting membrane (slope) conductance. The muscles were deprived of intracellular Cl by soaking them in a saline containing a relatively impermeant anion, and then they were exposed to varying extracellular salines for the measurements. Conductances were corrected for cation contributions by subtracting a control conductance measured in the presence of (presumably impermeant) cysteate anion. The second study (Bormann et al., 1987) was done on transmitter-activated Cl channels in mouse spinal neurons; here selectivity ratios were determined both from single-channel conductances in symmetrical salines and from whole-cell measurements of reversal potential under biionic conditions.

All of these Cl channels accept the halides and a variety of other anions. Halide permeabilities (from E_{rev}) increase from F to I, whereas conductances appear to peak for Cl. Our experiments with unilateral anion substitution (Fig. 8) also indicate that Br and I conductances, unlike their permeabilities, are fairly similar to that of Cl. The transmitter-activated channels reject F more strongly than the

channels of this article (an earlier study on transmitter-activated channels [Hamill et al., 1983] revealed F permeabilities close to that found in this article; it appears possible that the F-supported single-channel currents observed by Hamill et al. were due to the kind of channels studied here). Overall, the halide permeabilities of these channels follow the lyotropic pattern, with F as the least effective ion. Their conductances follow a different pattern, which suggests that the passage of halides other than Cl is slowed by binding to a channel site.

TABLE III

Selectivity Ratios Compared among Several Anion Channels

	G_m*	E_{rev}‡		γ‡		E_{rev}
	Skeletal muscle	Glycine receptor	GABA receptor	Glycine receptor	GABA receptor	This study
F		0.025	0.02			0.44
Cl	1	1	1	1	1	1
Br	0.58	1.4	1.5	0.74	0.88	1.46
I	0.28	1.8	2.8	0.85	0.82	1.98
SCN		7	7.3	0.54	0.75	1.44
Bicarbonate		0.11	0.18			
Phosphate			0.023			
Nitrate	0.44	1.9	2.1			2.35
Nitrite		1.4	1.5			
Formate	0.13–0.07	0.33	0.5			
Acetate	0.13–0.07	0.035	0.08			0.66
Proprionate	0.13–0.07		0.017			0.5
Trichloroacetate	0.17					
Benzoate	0.15					1.86
Valerate	0.13					
Butyrate	0.13–0.07					
Lactate	0.07					
Benzenesulfonate	0.05					
Isethionate	0.05					
Methylsulfonate	0.05					
Aspartate						0.17
Glutamate	0.02					0.13
Cysteate	0					

* From Woodbury and Miles (1973), who measured the resting Cl conductance of skeletal muscle using microelectrodes.

‡ From Bormann et al. (1987), who studied glycine and GABA receptor channels in cultured spinal cord neurons of embryonic mouse. These reversal potential measurements were done on whole cells; conductances were from single-channel recordings.

Permeabilities for nonhalide anions also match the lyotropic pattern. Thus, SCN and NO_3 are highly permeant in the neuronal channels. The channels in muscle and in our study reveal the tendency to accept organic anions with hydrophobic groups (benzoate) more readily than other anions of comparable size (e.g., glutamate). Hydrophobic interactions may be important in these channels. The permeabilities of the transmitter-activated channels reveal a fairly sharp cutoff with anion size that occurs between formate and acetate, whereas the other channels accept somewhat larger anions as well. The following pore

cross sections have been suggested to account for results with large anions: muscle, 5.5 × 6.5 Å^2 (on the basis of CPK models); glycine receptor, 5.2 Å diam; GABA receptor, 5.6 Å diam (on the basis of diffusion rates in a narrow cylinder). The CPK model of acetate, which is measurably permeant in the transmitter-activated channels, fits through a minimal cross section of ~4.0 × 5.0 Å^2. The largest permeant ions in our study would fit through a cross section of ~5.5 × 6.5 Å^2. Hence, the transmitter-activated channels may be slightly narrower than the others, but all channels must be considerably wider than the crystal diameter of a Cl anion (3.62 Å).

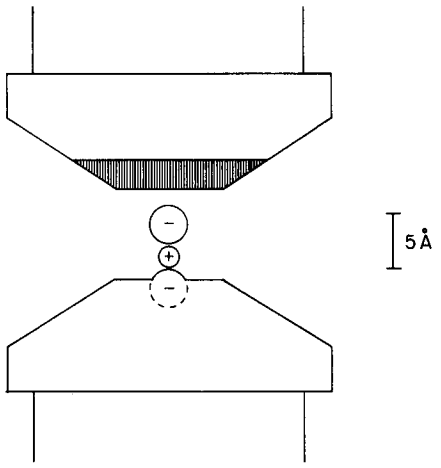

FIGURE 11. Schematic diagram of the proposed selectivity filter. The sizes of ions correspond to the crystal radii of Na and Cl ions. The dark part of the channel wall indicates a hydrophobic moiety. The space between this region and the adsorbed Na cation (5.5 Å) is large enough to admit all permeant anions in Table I; the larger organic anions, however, would have to align their long axes with the pore in order to pass, and they also require that the width of the channel in the direction vertical to the section shown be ~6.5 Å. The effective radius indicated for the anionic site of the pore is the crystal radius of a Cl anion. Ions are shown in the arrangement conforming to the activated complex; the complex may decay by releasing the anion or by releasing the cation/anion pair.

A Proposal for the Structure of the Selectivity Filter

We now attempt to combine the structural suggestions from the anion permeability measurements with a mechanism that could account for the dual anion and cation permeability in the neuronal anion channel. Our proposal is based on the simultaneous presence of anions and cations in the same channel and the resulting electrostatic interactions. We consider the simplest possible version, in which the channel has a single site.

The selectivity filter of the pore consists of an anionic group that is opposed by a hydrophobic moiety (Fig. 11). The anionic site attracts a monovalent cation from the bath such that it is occupied by a cation for most of the time. The

resulting dipole forms a weak cationic site, which in conjunction with the hydrophobic region forms a site suitable to accept a lyotropic anion. The activated complex of anionic site, cation, and anion can decay in two ways: by releasing the anion, or by releasing the cation-anion complex as a neutral pair. Anion flux then would imply anion association, followed by dissociation of the anion or the pair. Cation flux, in principle, could occur also in two ways: cation association and dissociation, or association of the cation, association of the anion, and then dissociation as a pair. We postulate that the pair mechanism for cation permeation prevails because the dissociation of a dipole from an anionic site requires less electrostatic work than the dissociation of a net cationic charge.

In order to accommodate the largest halide anion, I, the space left between the adsorbed cation and the channel walls has to be ~4.4 Å wide. Passage of a glutamate anion requires a minimal cross section of ~5.5 × 6.5 Å; this opening would pass all other anions found to be permeant. The blocker 9-ACA (Fig. 5*B*) would not pass.

In the Appendix, we formulate a flux equation for the proposed mechanism in terms of Eyring rate theory. With several simplifications that conform to the spirit of the mechanism outlined above, the *i-V* relationship is reduced to a function in two parameters (Eq. 1 of the Appendix): the association rate of the anion (acting like a scale factor to the current) and the ratio between the release rates for the anion and for the pair (this ratio determines the relative permeabilities for anions and cations). A reasonable prediction of the reversal potentials in Fig. 7 was obtained when the release rates for anions and pairs were equal (solid curve). The similarity of the two dissociation rates suggests that the effective anion radius of the channel's cation binding site is similar to that of the Cl ion (1.81 Å). When this site accepts an Na cation (0.95 Å), the resulting dipole would be sensed by a permeating anion as approximately equivalent to a single positive site of radius 5.52 Å. This is a low-field-strength site, which, on the basis of Eisenman's (1965) analysis, would conform to the observed halide selectivities. Cation permeation involves successive interactions with at least two charged species, the anionic site and a permeant anion, which could in principle account for the observation that the cation selectivity does not follow an Eisenman sequence. In addition to electrostatic forces, sterical constraints at the site of anion/cation interaction might be particularly important for the selectivities of this kind of channel, so one would not a priori expect to find Eisenman sequences.

We postulate that the conductance of the channel is limited by the association rate of anions. The theoretical analysis shows that this version of the mechanism produces the observed proportionality between conductance and salt activity. If, instead, the association of cation were the slowest step, the mechanism would predict a conductance that is independent of salt activity (because the rates of formation and decay of cation-site complexes are equally enhanced by increasing salt activity).

The species of cation present at the site should influence the permeability to anions. In comparing unitary currents in the presence of Cl and different alkali cations (Fig. 9), we found that Cs significantly enhances unitary conductance compared with Na, K, or Li.

The mechanism requires that a cation pass the channel only with the help of an anion. Hence, cation current should not be observed when suitable anions are unavailable. Indeed, we were unable to detect currents attributable to Na cation flux after replacing Cl with the impermeant SO_4 (Figs. 4 and 10). The model predicts that the membrane current would be positive at all membrane potentials while there is no permeant anion in the internal saline, and that current would be totally absent with impermeant anion on both sides, in agreement with our observations.

The anionic site, for which we estimate an effective radius similar to that of Cl, would represent a site of low electric field strength. Eisenman's (1962) inferences predict that a single site of this radius would preferentially attract the large alkali cations; affinities to divalent cations should be very low. Indeed, Ca and Mg at a concentration of 1 mM do not affect the selectivity of the channel (Table II). On the other hand, Zn blocks at this concentration (Fig. 5*A*), which suggests a specific interaction between Zn and the channel. These findings parallel those obtained for the resting Cl conductance of skeletal muscle (Hutter and Warner, 1967*b*; Woodbury and Miles, 1973). The Cl conductance of muscle, in addition to its sensitivity to Zn, is reduced in the presence of a low pH (Hutter and Warner, 1967*a*; Woodbury and Miles, 1973). Both the Zn and proton blocks have been suggested to arise from binding to a histidyl residue within the muscle Cl channel. The observation that the channel conductance drops when the activity of these cations is increased appears to be consistent with the mechanism proposed in this article: association of the channel with a Zn or H ion is likely to prevent the adsorption of a cation species that promotes anion permeation.

The permeation mechanism we propose for the neuronal anion channels can be compared with a mechanism previously suggested for amphotericin B channels (Borisova et al., 1986). There, an extrinsic anion adsorbed to a cationic site has been suggested to allow the passage of extrinsic cations, whereas we postulate here the converse scheme, in which adsorption of cations to an anionic site forms the passage for anions. Although in both mechanisms cation permeation is abolished by the absence of suitable anions, two other observations make the amphotericin B mechanism unlikely to apply to the neuronal channel. (*a*) It requires anions to be bound in order to pass cations. Whereas the unitary conductance of amphotericin B channels is half-saturated at NaCl concentrations near 100 mM, the conductance-concentration curve of the neuronal channel does not saturate up to 1 M. If the conductances reflect the binding of the main charge carrier, the anion, similar anion/cation selectivity ratios in these two kinds of channel would imply that the anion-containing neuronal channel passes cations at a much higher rate than that possible in the amphotericin B channel. (*b*) The unitary conductance of the neuronal channel varies with the species of cation present. This is hard to explain if the passage of anion does not imply some interaction with a bound cation.

Physiological Role of the Anion Channel

From the finding that the anion channel is significantly permeable also to cations, one might expect that it has a destabilizing, rather than the usually anticipated

stabilizing, effect on the membrane potential. We cannot test this point experimentally, since the unitary currents under conditions comparable to those of a resting cell are too small to be measured, but we can use the permeation model derived from the experiments described before in order to predict the physiological effect of the channel. In contrast to a mechanism where anions and cations pass independently of each other, the mechanism suggested by our experiments has the remarkable property that, in the absence of a concentration gradient for cations, the reversal potential is determined solely by anions. This can be readily verified by inspection of Eq. 1 of the Appendix. Since the channel apparently does not discriminate between Na and K ions (Table I), it does not experience a significant cation activity gradient under physiological conditions. Hence, its reversal potential depends on the activities of permeant anions in nearly the same way as it would for a purely anion-selective channel. To the extent that Cl is the major permeant anion in the cell environment, this anion channel could help stabilize the membrane potential near the negative limit of the physiological range. While the channel's ability to pass cations would not be expressed in the net current, it would produce a small net flux of NaCl into the resting cell.

In terms of whole-cell behavior, the net electrical effect of this anion channel can be expected to mimic that of a slow, delayed rectifier K channel. What actual physiological functions the channel may have in the neurons remains to be elucidated. The density and the ionic permeability of the channel suggest that it is an important factor in stabilizing a negative membrane potential.

APPENDIX

In the following, we derive an *i-V* relationship for the mechanism illustrated in Fig. 11. We define three equilibrium states: (1) no extrinsic ion is bound; (2) only a cation is bound; (3) a cation and an anion are bound. Of the possible transitions among these states, we exclude (*i*) the dissociation of the cation (state 2 leads to state 1), and (*ii*) the association of an ion pair (state 1 leads to state 3). The first transition is excluded because dissociation of the cation is considered unlikely (cations dissociate in the form of ion pairs). The second transition implies a trimolecular reaction step, whose rate is taken as negligible. We introduce the notation k'_{12} for the transition that converts state 1 into state 2 by association of a cation through the cytosolic mouth of the channel, c'_+, for the cation concentration in the cytosol, c''_-, for the anion concentration in the extracellular bath, and so on. In the stationary state, occupancies of the three states, p_1, p_2, and p_3, obey, in matrix notation:

$$\begin{bmatrix} -a_{11} & 0 & a_{13} \\ a_{11} & -a_{22} & a_{23} \\ 1 & 1 & 1 \end{bmatrix} \times \begin{bmatrix} p_1 \\ p_2 \\ p_3 \end{bmatrix} = \begin{bmatrix} 0 \\ 0 \\ 1 \end{bmatrix}$$

where $a_{11} = k'_{12}\, c'_+ + k'_{12}\, c''_+$; $a_{13} = k'_{31} + k''_{31}$; $a_{22} = k'_{23}\, c'_- + k''_{23}\, c''_-$; and $a_{23} = k'_{32} + k''_{32}$. The cation flux at the cytosolic mouth of the channel is:

$$\Phi_+ = p_1\, k'_{12}\, c'_+ - p_3\, k'_{31}.$$

The anion flux is:

$$\Phi_- = p_2\, k'_{23}\, c'_- - p_3\, k'_{32} - p_3\, k'_{31}.$$

The current is the difference of the two fluxes, scaled by the Faraday:

$$I = F(\Phi_+ - \Phi_-).$$

We assume that all rate constants in the absence of a transmembrane voltage are the same for corresponding reactions at either side of the channel, and describe the voltage dependence of rates that imply movement of ions using the Boltzmann factor:

$$B(d) = \exp(dFE/RT),$$

where E is the transmembrane voltage (inside minus out), and R and T have their usual meaning. For simplicity, we place the ion-binding site in the electric center of the membrane and barrier peaks for ion movements halfway between the center and the mouths. Then, $k'_{12} = k_{12}\,B(1/4)$; $k''_{12} = k_{12}\,B(-1/4)$; $k'_{23} = k_{23}\,B(-1/4)$; $k''_{23} = k_{23}\,B(1/4)$; $k'_{32} = k_{32}\,B(1/4)$; $k''_{32} = k_{32}\,B(-1/4)$; $k'_{31} = k''_{31} = k_{31}$. Finally, we postulate that the cation association rate, k_{12}, is much larger than all other rates, and that the anion adsorption rate, k_{23}, is much smaller than all other rates. After taking the appropriate limits of the current equation, we obtain the i-V relationship:

$$I(E) = F\,k_{23}\,\frac{N_- + N_{+-}}{D}, \tag{1}$$

where $N_- = [B(1/4)\,c'_+ + B(-1/4)\,c''_+][B(1/2)\,c''_- - B(-1/2)\,c'_-]$; $N_{+-} = 2(k_{31}/k_{32})[B(1/2)\,c'_+ c''_- - B(-1/2)\,c''_+ c'_-]$; $D = [B(1/4)\,c'_+ + B(-1/4)\,c''_+][2(k_{31}/k_{32}) + B(1/4) + B(-1/4)]$. The numerator term N_- becomes zero if there is no charge transfer involving the anion dissociation mechanism; the term N_{+-} disappears when there is no charge transfer involving ion pair dissociation. Note that membrane current is governed by two parameters, a scaling factor to the current, and the ratio of two dissociation rates, for anions and for ion pairs. In the absence of a permeant anion, both numerator terms, and hence the current, become zero. With equal cation activities on the two sides, the reversal potential of the current becomes identical to the Nernst potential for the anion.

We thank Dr. John Barrett and Ms. Doris Nonner for their generous help in growing neuron cultures, Dr. Theodore Kehl and his staff for providing computer resources, and Drs. David Adams and Ellen Barrett for reading a draft of the manuscript. We are grateful to C. Freites and J. Gray for building the mechanical and electronic equipment.

This work was supported by grant GM-30377 from the National Institutes of Health.

Original version received 10 November 1986 and accepted version received 15 June 1987.

REFERENCES

Blatz, L. A., and K. L. Magleby. 1983. Single voltage-dependent chloride-selective channels of large conductance in cultured rat muscle. *Biophysical Journal.* 43:237–241.

Blatz, L. A., and K. L. Magleby. 1984. Ion conductance and selectivity of single calcium-activated potassium channels in cultured rat muscle. *Journal of General Physiology.* 84:1–23.

Blatz, L. A., and K. L. Magleby. 1985. Single chloride-selective channels active at resting membrane potentials in cultured rat skeletal muscle. *Biophysical Journal.* 47:119–123.

Borisova, M. P., R. A. Brutyan, and L. N. Ermishkin. 1986. Mechanism of anion-cation selectivity of amphotericin B channels. *Journal of Membrane Biology.* 90:13–20.

Bormann, J., O. P. Hamill, and B. Sakmann. 1987. Mechanism of anion permeation through channels gated by glycine and γ-aminobutyric acid in mouse cultured spinal neurones. *Journal of Physiology.* 385:243–286.

Brugge, J. S., P. C. Cotton, A. E. Queral, J. N. Barrett, D. Nonner, and R. W. Keane. 1985. Neurons express high levels of a structurally modified, activated form of pp60$^{c\text{-}src}$. *Nature.* 316:554–557.

Bryant, S. H., and A. Morales-Aguilera. 1971. Chloride conductance in normal and myotonic

muscle fibers and action of monocarboxylic aromatic acids. *Journal of Physiology.* 219:367–383.

Dani, J. A., J. A. Sanchez, and B. Hille. 1983. Lyotropic anions. Na channel gating and Ca electrode response. *Journal of General Physiology.* 81:255–281.

Eisenman, G. 1962. Cation selective glass electrodes and their mode of operation. *Biophysical Journal.* 2:259–323.

Eisenman, G. 1965. Some elementary factors involved in specific ion permeation. *Proceedings of the XXIIIrd International Congress of Physiological Sciences.* 87:489–506.

Eisenman, G., and R. Horn. 1983. Ionic selectivity revisited: the role of kinetic and equilibrium processes in ion permeation through channels. *Journal of Membrane Biology.* 76:197–225.

Franciolini, F., and W. Nonner. 1986. Permeability of anion channels in rat hippocampal neurons. *Biophysical Journal.* 49:414*a*. (Abstr.)

Gray, P. T. A., S. Bevan, and J. M. Ritchie. 1984. High conductance anion-selective channels in rat cultured Schwann cells. *Proceedings of the Royal Society of London, Series B.* 221:395–409.

Hamill, O. P., J. Bormann, and B. Sakmann. 1983. Activation of multiple-conductance state chloride channels in spinal neurones by glycine and GABA. *Nature.* 305:305–309.

Hamill, O. P., A. Marty, E. Neher, B. Sakmann, and F. J. Sigworth. 1981. Improved patch-clamp techniques for high-resolution current recording from cells and cell-free membrane patches. *Pflügers Archiv.* 391:85–100.

Hofmeister, F. 1890. Zur Lehre von der Wirkung der Salze. Fünfte Mittheilung. Untersuchungen über den Quellungsvorgang. *Archiv für Experimentelle Pathologie und Pharmakologie.* 27:395–413.

Hutter, O. F., and A. E. Warner. 1967*a*. The pH sensitivity of the chloride conductance of frog skeletal muscle. *Journal of Physiology.* 189:403–425.

Hutter, O. F., and A. E. Warner. 1967*b*. Action of some foreign cations and anions on the chloride permeability of frog muscle. *Journal of Physiology.* 189:445–460.

Kaufman, L. M., and J. N. Barrett. 1983. Serum factor supporting long-term survival of rat central neurons in culture. *Science.* 220:1394–1396.

Miller, C., and M. M. White. 1984. Dimeric structure of single chloride channels from *Torpedo* electroplax. *Proceedings of the National Academy of Sciences.* 81:2772–2775.

Palade, P. T., and R. L. Barchi. 1977. On the inhibition of muscle membrane chloride conductance by aromatic carboxylic acids. *Journal of General Physiology.* 69:879–896.

Robinson, R. A., and R. H. Stokes. 1959. Electrolyte Solutions. 2nd ed. Butterworth, London. 491–500.

Rosenberg, P. A., and A. Finkelstein. 1978. Interaction of ions and water in gramicidin A channels. *Journal of General Physiology.* 72:327–340.

Stanfield, P. R. 1970. The differential effects of tetraethylammonium and zinc ions on the resting conductance of frog skeletal muscle. *Journal of Physiology.* 209:231–256.

Woodbury, J. W., and P. R. Miles. 1973. Anion conductances of frog muscle membranes: one channel, two kinds of pH dependence. *Journal of General Physiology.* 62:324–353.